Superlattices and Microstructures 36 (2004) 537–545

Superlattices
and Microstructures

www.elsevier.com/locate/superlattices

Structural and optical characterisation of InN layers grown by MOCVD

P. Singh[a,*], P. Ruterana[a], M. Morales[a], F. Goubilleau[a],
M. Wojdak[b], J.F. Carlin[c], M. Ilegems[c], D. Chateigner[d]

[a] *SIFCOM, UMR 6176 CNRS-ENSICAEN, Université de Caen, 6 Bd du Maréchal Juin, 14050 Caen Cedex, France*
[b] *CIRIL, UMR 6637 CNRS-ENSICAEN, Université de Caen, 6 Bd du Maréchal Juin, 14050 Caen Cedex, France*
[c] *IPEQ, Ecole Polytechnique Fédérale de Lausanne, CH-1015 Lausanne, Switzerland*
[d] *CRISMAT, UMR 6508 CNRS-ENSICAEN, 6 Bd Maréchal Juin, 14050 Caen, France*

Abstract

In the following, we report investigations of the dependencies of the structural, optical and electrical characteristics of InN thin films grown by MOCVD on the growth temperature. The layer thicknesses range from 70 to 400 nm. Their carrier concentrations range from 7×10^{18} to 4×10^{19} cm^{-3}. Hall mobility values from 150 to 1300 cm^2/V/s were determined in these films. The variation of the growth temperature and V/III ratio brought about different growth modes and rates. Using TEM, in addition to measuring layer thickness, we also determined the growth mode along with the structural quality of the InN layers. The surface roughness was obtained from AFM measurements. The layer crystalline quality was also investigated by means of X-ray diffraction in the rocking mode. Photoluminescence measurements performed at room temperature and at 7 K gave emission at around 0.7 eV.

1. Introduction

InN is seen as a material which will be suitable for use in fabricating LEDs, LDs and ultrahigh frequency transistors [1]. It is part of the nitride semiconductor family along with

---

[*] Corresponding author.
E-mail address: protima.singh@ismra.fr (P. Singh).

0749-6036/$ - see front matter © 2004 Elsevier Ltd. All rights reserved.
doi:10.1016/j.spmi.2004.10.002

Table 1
MOCVD growth conditions of the InN samples

Sample	Growth temperature (°C)	V/III ratio	GT (h)	NH_3 flow (sccm)	In flow (sccm)	Aspect
A50	550	13 000	3.5	3000	50	Black/brown
A52	650	6 500	1.25	3000	100	Black/brown
A53	500	6 500	2	3000	100	Metallic brown
A65	575	3 300	–	3000	200	Black brown/In drops
A69	450	3 300	1.5	3000	200	Metal In drops
A70	450	6 500	1.5	6000	200	Metallic yellow

AlN, GaN and their alloys. InN exhibits the smallest effective mass and the highest electron drift velocity as compared to the rest of the nitride family [2]. However, its growth is more difficult to achieve than that of AlN and GaN due to the weak bonding of In and N [3]. Nevertheless, over the past two years, using MBE and MOCVD as growth techniques has greatly improved the quality of InN films and recent reports on the band gap show that it could be as small as 0.65 eV [4].

2. Experimental

The InN layers investigated were grown on a (0001) sapphire substrate followed by a 500 to 1000 nm thick GaN template. The growth temperature was varied from 475 to 650 °C while the V/III ratio ranged from 13 000 to 3300 (Table 1). Since the growth temperature is one of the dominant factors as regards the quality of these films, we tried to correlate it with a number of measurements starting with the surface roughness obtained from AFM over area scans of 5 μm × 5 μm and down to 1 μm × 1 μm. The PL measurements were carried out on all the samples using a Sa:Ti laser at low temperature (7 K) and at room temperature, the pump power used was 500 mW and the excitation wavelength was 781 nm. We also carried out TEM analysis on our JEOL 2010 analytical microscope operated at 200 kV. X-ray diffraction investigation was performed by recording the (0002) rocking curves and exploring the reciprocal lattice from 0° to 60° and 0° to 360° using ψ and χ scans, respectively. This was done to investigate the epitaxial relationships of the layers and to measure the half-width half-maxima of the main out-of-plane peaks.

3. Results

3.1. Surface roughness investigation by AFM

Fig. 1 shows typical topological (area of 5 μm × 5 μm) and phase images (area of 1.5 μm × 1.5 μm) from AFM measurements for the three samples grown at 650 °C (A52), 575 °C (A65), 450 °C (A70). The sample A52 at this micron scale (Fig. 1(a)) has a surface structure with large separated peaks. The phase image (Fig. 1(d)) of this sample for a smaller scan area shows mostly four-sided grains of various shapes. A65 (Fig. 1(b)) has peaks which are pointed too, but they seem to be almost joined, indicating a continuous

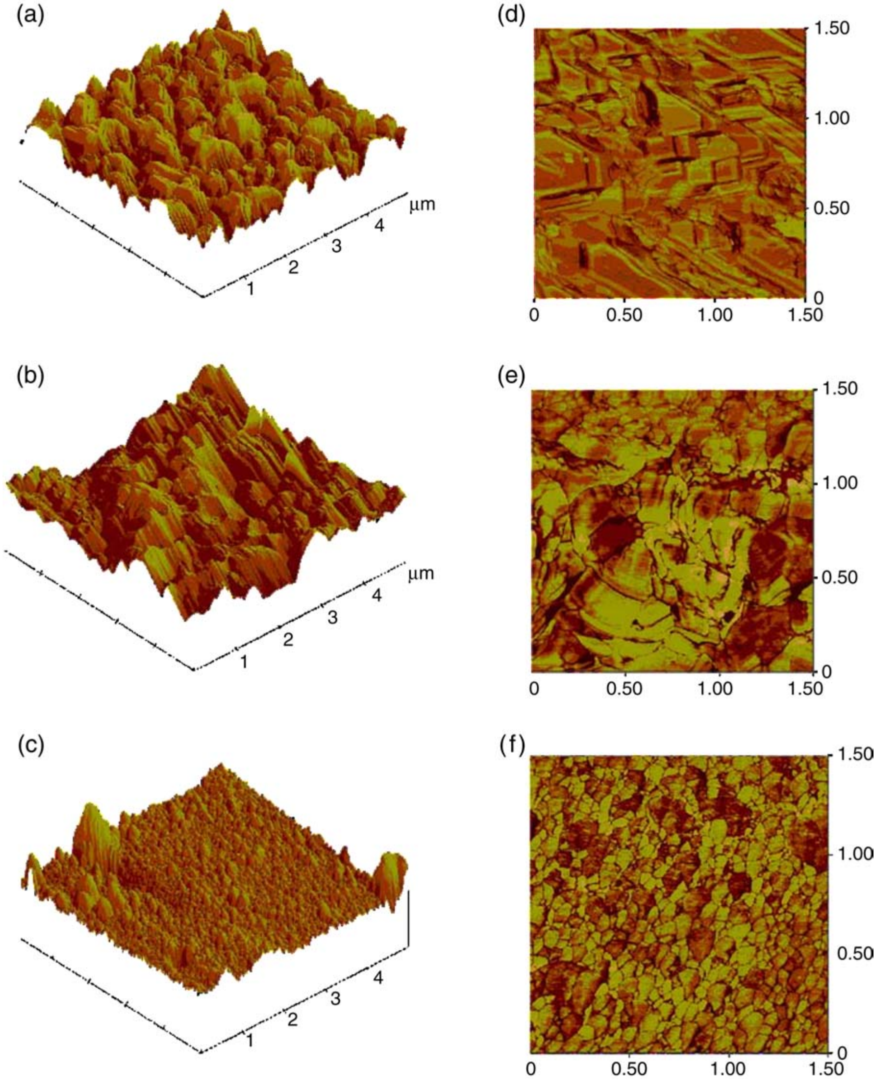

Fig. 1. AFM ((a), (b), (c)) topological images and ((d), (e), (f)) phase images of samples A52, A65, A70 respectively.

layer below. Its phase image (Fig. 1(e)) shows grains that are curved and fit into their neighbours. It is also observed that the grains are larger compared to those of A52. For A70 (Fig. 1(c)), the small peaks have rounded off slopes that almost touch each other, hinting at the presence of a continuous layer. In its phase image (Fig. 1(f)) there are tiny grains which form clusters. This sample had the smallest grains among the three presented here.

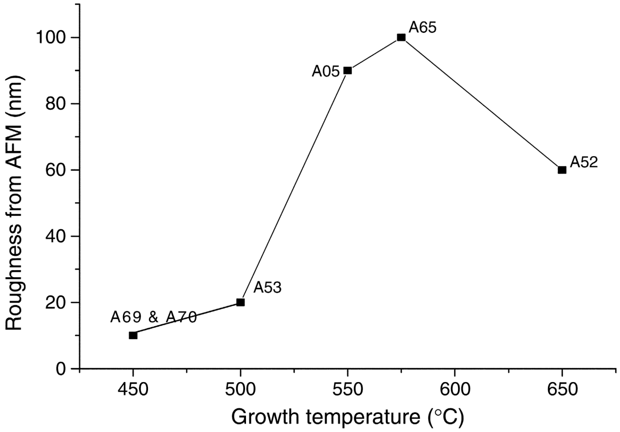

Fig. 2. Roughness obtained from AFM studies as a function of growth temperature.

In Fig. 2, the roughness is plotted versus the growth temperature for the samples investigated. A69 and A70 grown at the same growth temperature of 450 °C have the same roughness. From 450 to 500 °C the roughness increases by only 10 nm. However, from 500 to 550 °C it jumps by 65 nm in a temperature span of 50 °C. From 550 to 575 °C the roughness increases by 15 nm. Finally, the roughness falls by 40 nm from 575 to 650 °C or when close to the InN dissociation temperature.

3.2. *Layer quality and thickness determination by TEM*

Although all the samples shown in Table 1 have been observed by TEM, we concentrate on three samples out of which two were discussed above in relation to AFM measurements. Fig. 3 shows bright field images of the three samples. A52 (Fig. 3(a)) has pointed and sharp peaks, but, towards the interface, the islands are coalesced. This morphology is in agreement with the above AFM images where we also find sharp peaks which are separated. A50 (Fig. 3(b)) grown at 550 °C has almost coalesced islands with flat tops; this probably indicates that we may be close to the growth conditions from which the growth of a coalescence layer can be initiated. A70 (Fig. 3(c)) exhibits pointed peaks but it appears more continuous than A52. If we compare the morphology of the three samples we find that for A52 and A70 have the same V/III ratio, their layers are similar and A70 is more continuous than A52. The layer discontinuity for A52 is attributed to the higher temperature of 650 °C (dissociation temperature for InN) giving a higher growth rate of 0.29 μ/h in comparison to 0.05 μ/h for A70.

As a general trend the growth rate increases with the growth temperature (Fig. 4). In our case the In flow was reduced by half every 50 °C rise in temperature from 450 to 550 °C; nevertheless, there was an increase in the growth rate and at a growth temperature of 650 °C for A52 a growth rate as high as 0.29 μ/h is obtained. Adachi et al. report that the growth rate of InN increased with increasing temperature from 450 to 550 °C, even when the V/III ratio was constant and saturated, when the TMI flow was increased, as excess of In does not form InN bonds limited by NH_3 decomposition or due to the deficiency of

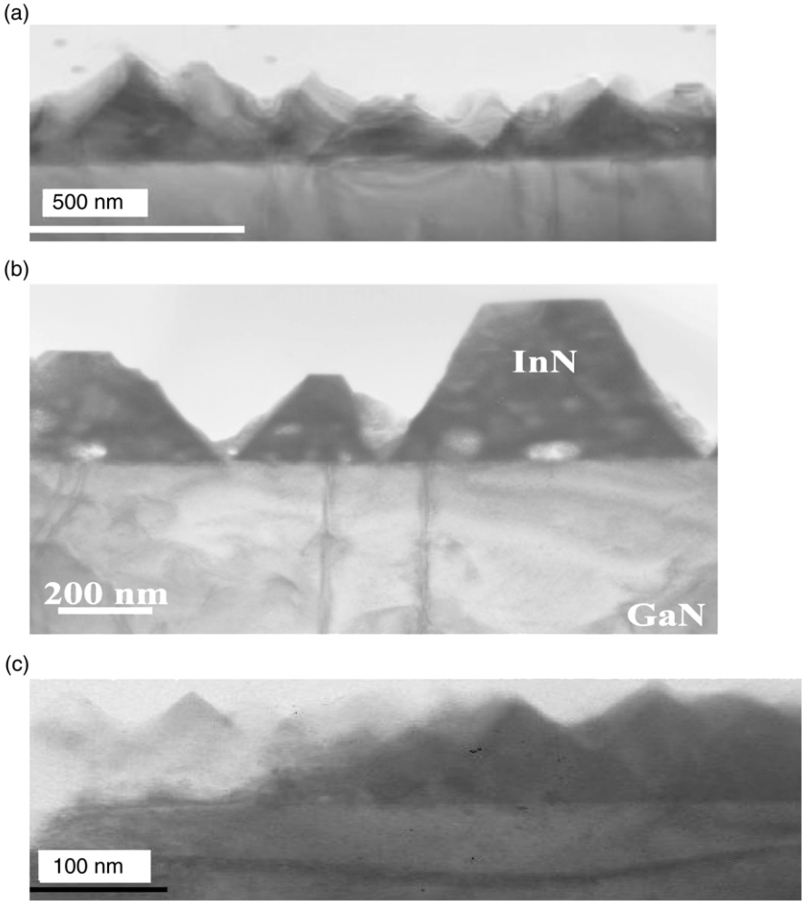

Fig. 3. TEM images of (a) A52, (b) A50, (c) A70.

active nitrogen [5]. At 630–650 °C the growth rate is directly proportional to the V/III ratio due to enhanced decomposition of NH_3 and a growth rate as high as 0.8 μ/h is obtained at 650 °C [5].

3.3. X-ray diffraction analysis

X-ray diffraction analysis was performed by recording the (0002) rocking curves in order to obtain mosaicity of the growth along the (0001) axis. By exploring the reciprocal lattice from 0 to 60° and 0 to 360°, i.e. using ψ and χ scans, we confirmed the following epitaxial relationships: $[11\bar{2}0]_{\text{Sapphire}} \parallel [10\bar{1}0]_{\text{InN\&GaN}}$, $[10\bar{1}0]_{\text{Sapphire}} \parallel [11\bar{2}0]_{\text{InN\&GaN}}$ in agreement with TEM diffraction analysis. The above technique was used also to measure the out-of-plane half-widths at half-maxima (HWHM) $\Delta\phi$ of the main InN peaks, thus enabling us to study the crystalline quality of the InN grains (Table 2). Fig. 5 is a plot of $\Delta\phi$ versus the growth temperature. A50 and A53 have almost the same value of

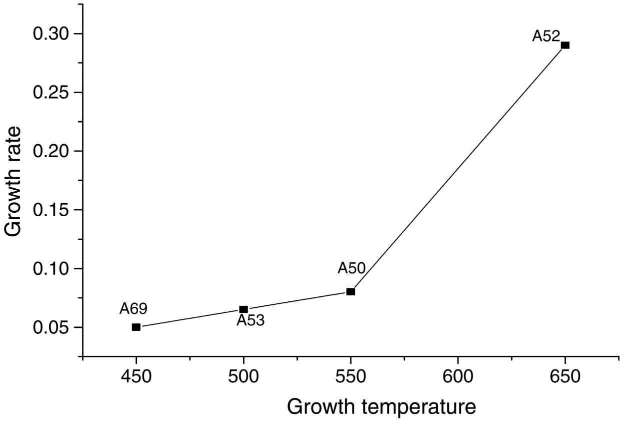

Fig. 4. Growth rate as a function of growth temperature.

Table 2
Asymmetrical 103 and 104 peak positions and half-widths at half-maxima

	103 InN			103 GaN			104 Al_2O_3		
χ_{max} (°)	32	31.85	31.66	32.12	31.98	32.019	–	–	–
$\Delta\chi$ (°)	0.77	1.2	0.78	0.66	0.65	0.665	–	–	–
φ_{max} (°)	17.92	17.69	17.79	17.86	18.02	18.12	48.147	48.3	47.64
$\Delta\varphi$ (°)	0.395	1.70	0.365	0.25	0.25	0.24	0.16	0.15	0.16
Films	A50	A52	A53	A50	A52	A53	A50	A52	A53

HWHM. However, for A52 it increases by 1.4°. Nanishi et al. reported that a large HWHM is due to the presence of tilted domains along the (0002) direction. These tilted domains give rise to stacking faults and dislocations which are known to degrade the electrical and optical properties of the films. We have taken into account the fact that this sample was grown at a temperature of 650 °C which is the dissociation temperature for InN. This implies that there are In aggregates which degrade the crystalline quality of these films [5].

3.4. Photoluminescence

PL measurements were made on all the samples at 7 K and room temperature. Samples A65, A69 and A70 showed no luminescence at all. Among the three samples the minimum and maximum PL emission peaks were centred at 0.68 eV at 7 K and at 0.78 eV for room temperature measurements. The PL spectra for these samples are shown below in Fig. 6a. We find that A52 has the smallest PL band gap; in principle we should have A50 giving the smallest PL band gap because of its good crystalline structure and high mobility. However it does have the most intense signal. A53 and A52 have a PL intensity less than A50 (Fig. 6a). In addition to that, the PL intensity decreases as the crystalline quality decreases. A plot of PL intensity at 7 K and at room temperature versus growth temperature is shown

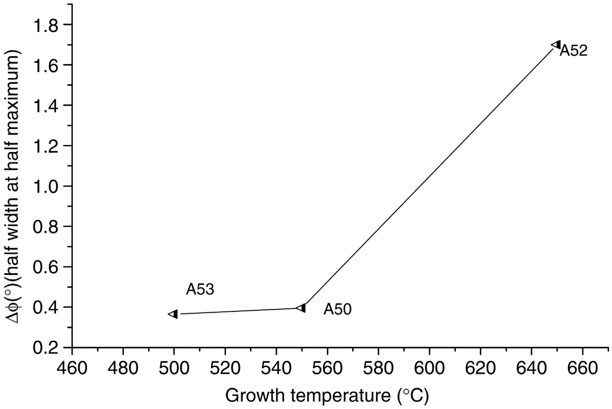

Fig. 5. HWHM ($\Delta\phi$) as a function of growth temperature.

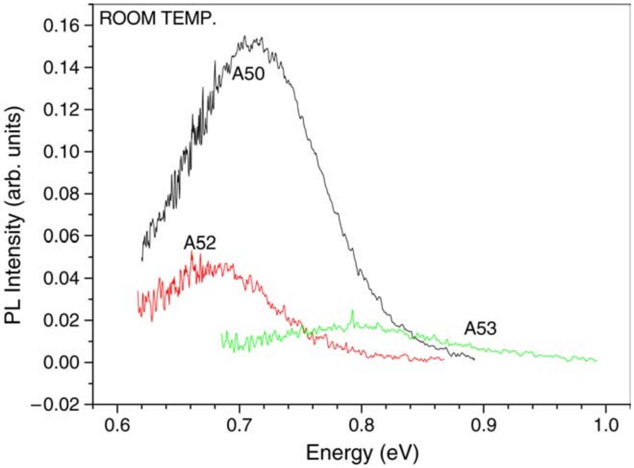

Fig. 6a. Photoluminescence spectra of the samples at room temperature.

in Fig. 6b. It can be noted that the peak position shifts to higher energy with increasing growth temperature [6].

Fig. 6c is the plot of band gap versus carrier concentration. A50 which gives the most intense signal has the lowest carrier concentration (along with A52) due to its rather good crystalline quality, which comes from it being prepared at high temperature (below the InN dissociation temperature) with a high V/III ratio—whereas A53 which has the least intense signal has also the highest carrier concentration due to its lower growth temperature and lower V/III ratio indicating poorer crystalline quality. A52 having the smallest PL band gap gave the least intense signal even though it had the same carrier concentration as A50.

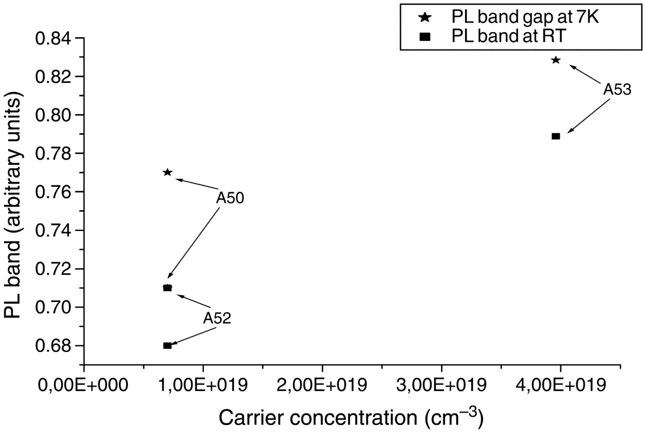

Fig. 6b. PL band gaps of the samples obtained at room temperature and at 7 K as a function of growth temperature.

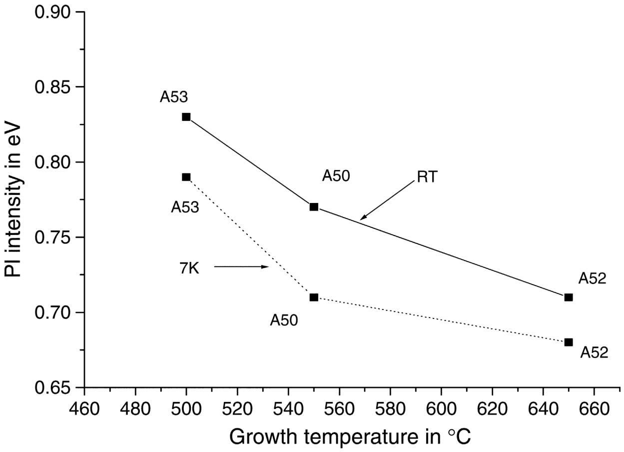

Fig. 6c. PL peak position as a function of carrier concentration.

3.5. Hall mobility

Fig. 7 is a plot of Hall mobility versus growth temperature. A50 exhibits the highest hall mobility of 1300 cm^2/V/s which is higher than that of A53. High V/III ratio or low In flow used during the growth along with temperature rise have been reported to significantly improve the electrical properties due to the filling up of nitrogen vacancies [7]. Moreover, as shown above, it is of good crystalline quality and has a low carrier concentration. A52 on the other hand had a small Hall mobility and as seen from the above this is due to its low crystalline quality (dissociation of the InN bond).

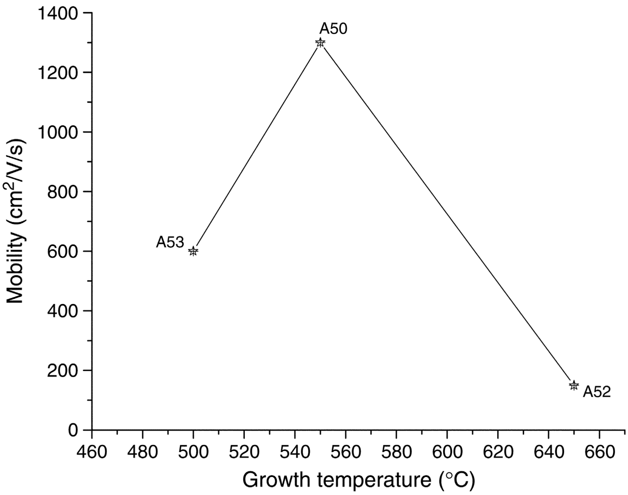

Fig. 7. Hall mobility as a function of growth temperature.

4. Conclusion

We have studied MOCVD samples prepared below the InN dissociation temperature (450–575 °C) and at the InN dissociation temperature 650 °C. On the other hand, A52 prepared at the InN dissociation temperature (650 °C), even though it had a lower roughness, the same carrier concentration as A50 and a smaller PL band gap, had a very small PL signal and Hall mobility which is an indication of its poor crystalline quality. In this case thermal decomposition of the InN layer governs the electrical properties [8]. Among the samples grown below the dissociation temperature, A50 which was grown at 550 °C had the best optical and electrical properties with flat topped islands. This can probably be attributed to its optimum growth temperature and V/III ratio which improved its Hall mobility.

References

[1] S.C. Jain, M. Willander, J. Narayan, R.V. Overstraeten, J. Appl. Phys. 87 (2000) 965.
[2] A.G. Bhuiyan, A. Hashimoto, A. Yamamoto, J. Appl. Phys. 94 (2003) 2779.
[3] V.Yu. Davydov, A.A. Klochikhin, R.P. Seisyan, V.V. Emstev, S.V. Ivanov, F. Bechstedt, J. Furthmüller, H. Harima, A.V. Mudryi, J. Aderhold, O. Semchinova, J. Graul, Phys. Status Solidi b 229 (2002) R1.
[4] M. Adachi, Y. Murakami, A. Hashimoto, A. Yamamoto, Proceedings of the International Workshop on Nitride Semiconductors, IWN'2000, Nagoya, Japan, September 24–27, IPAP Conference Series, vol. 1, 2000, p. 339.
[5] A. Koukitu, T. Taki, N. Takahashi, H. Seki, J. Cryst. Growth 197 (1999) 99.
[6] Y. Nanishi, Y. Saito, T. Yamaguchi, F. Matsuda, T. Araki, H. Naoi, A. Suzuki, H. Harima, T. Miyajima, Mater. Res. Soc. Symp. 798 (2004) Y12.1.1.
[7] A. Yamamoto, Y. Murukami, K. Koide, M. Adachi, A. Hashimoto, Phys. Status Solidi b 228 (2001) 5.
[8] V. Davydov, A. Khlochikin, S. Ivanov, J. Aderhold, A. Yamamoto, Nitride semiconductors, in: P. Ruterana, M. Albrecht, J. Neugebauer (Eds.), Hand Book on Materials and Devices, 2003, p. 274.